AD-A148 655 VOLTAMMETRY AND COULOMETRY WITH IMMERSED THIN LAYER ELECTRODES PART 1 MOD.. (U) UTAH UNIV SALT LAKE CITY DEPT OF CHEMISTRY A S HINMAN ET AL. 28 NOV 84 TR-30 1/1

UNCLASSIFIED N00014-83-K-0470 F/G 7/4 NL

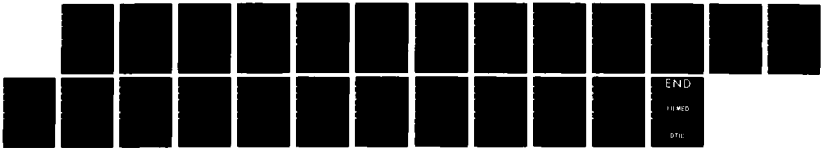

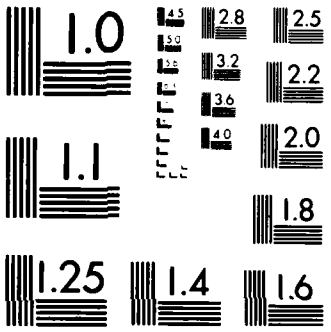

(12)

OFFICE OF NAVAL RESEARCH

Contract N00014-83-K-0470

Task No. NR 359-718

TECHNICAL REPORT NO. 30

Voltammetry and Coulometry with Immersed Thin Layer Electrodes. Part I. Model for Effects of Solution Resistivity in Linear Sweep Voltammetry.

By

A. Scott Hinman
Stanley Pons
John Cassidy

Prepared for Publication in

Electrochim. Acta

University of Utah
Department of Chemistry
Salt Lake City, Utah 84112

November 28, 1984

SECURITY CLASSIFICATION OF THIS PAGE (When Data Entered)

REPORT DOCUMENTATION PAGE	READ INSTRUCTIONS BEFORE COMPLETING FORM
1. REPORT NUMBER: 30	2. GOVT ACCESSION NO.: AD A148 655
	3. RECIPIENT'S CATALOG NUMBER:
4. TITLE (and Subtitle): Voltammetry and Coulometry with Immersed Thin Layer Electrodes. Part I. Model for Effects of Solution Resistivity in Linear Sweep Voltammetry	5. TYPE OF REPORT & PERIOD COVERED: Technical Report # 30
	6. PERFORMING ORG. REPORT NUMBER:
7. AUTHOR(s): A. Scott Hinman; Stanley Pons*; John Cassidy	8. CONTRACT OR GRANT NUMBER(s): N00014-83-K-0470
9. PERFORMING ORGANIZATION NAME AND ADDRESS: University of Utah, Department of Chemistry, Salt Lake City, UT 84112	10. PROGRAM ELEMENT, PROJECT, TASK AREA & WORK UNIT NUMBERS: Task No. NR 359-718
11. CONTROLLING OFFICE NAME AND ADDRESS: Office of Naval Research, Chemistry Program - Chemistry Code 472, Arlington, Virginia 22217	12. REPORT DATE: November 28, 1984
	13. NUMBER OF PAGES: 21
14. MONITORING AGENCY NAME & ADDRESS (if different from Controlling Office)	15. SECURITY CLASS. (of this report): Unclassified
	15a. DECLASSIFICATION/DOWNGRADING SCHEDULE

16. DISTRIBUTION STATEMENT (of this Report)

This document has been approved for public release and sale; its distribution unlimited.

17. DISTRIBUTION STATEMENT (of the abstract entered in Block 20, if different from Report)

18. SUPPLEMENTARY NOTES

19. KEY WORDS (Continue on reverse side if necessary and identify by block number)

Voltammetry, thin layer electrochemistry

20. ABSTRACT (Continue on reverse side if necessary and identify by block number)

none

DD FORM 1473 EDITION OF 1 NOV 65 IS OBSOLETE
S/N 0102-LF-014-6601

Unclassified
SECURITY CLASSIFICATION OF THIS PAGE (When Data Entered)

Voltammetry and Coulometry with Immersed Thin Layer Electrodes. Part I. Model for Effects of Solution Resistivity in Linear Sweep Voltammetry

A. Scott Hinman
Department of Chemistry
University of Calgary
Calgary, Alberta
CANADA

Stanley Pons,* and John Cassidy
Department of Chemistry
University of Utah
Salt Lake City, Utah 84112
U.S.A.

* To whom all correspondence should be addressed.

INTRODUCTION

Before any attempt can be made to quantitatively analyze a voltammetric wave, or any inference concerning the nature of the product of a heterogeneous charge transfer process can be drawn, the number of electrons, n, associated with the underlying redox process must be known. A number of voltammetric critieria (1) can be applied to this end provided that the associated charge transfer process is reversible: i.e., no homogeneous reactions are coupled to the heterogeneous charge transfer, and the standard heterogeneous rate constant, k_s, is large enough that the Nernst equation can be used to calculate the concentrations of the two forms of the redox couple. If this is not the case, then some method other than the application of standard voltammetric criteria must be used. This is most often controlled potential coulometry (2).

The procedure employed in controlled potential coulometry generally involves applying a constant potential to the working electrode and allowing current to flow until it has decayed to within a few percent of its initial value, or until no further decay of the current with time is observed. The total charge passed during this time is then assumed to correspond to that required for complete electrolysis. In most conventional coulometric cell designs, such an experiment requires several hours to complete, and the precision with which n-values may be determined is often not good. The procedure is especially disadvantageous when working with organic systems where solvents or electroactive species are difficult to purify or are available

in limited quantity. When working at potentials near the anodic or cathodic limits of the solvent, or when the electrolysis products are of limited stability, the current may never decay to background levels. Under such circumstances it is extremely difficult to be objective in determining an electrolysis endpoint. The poor potential distribution across the working electrode surface which is encountered in many coulometric cell designs is particularly pronounced when working in non-aqueous solvents, and may prohibit the determination of n for a particular voltammetric wave when this is not well separated in potential from other voltammetric processes.

In aqueous systems, thin layer electrochemistry (3) offers a very attractive alternative to controlled potential coulometry for n-value measurement. Here, a very small volume of solution is confined to a thin layer (2-50 μm) next to the electrode surface. Complete electrolysis of the electroactive species can then be achieved in very short time periods (ca 1 sec.). Diffusion of electroactive species within the thin layer may often be ignored in theoretical treatments, and the resulting equations are especially simple and easy to interpret. The peak currents in thin layer voltammetry theoretically occur at the formal redox potential, and this fact, in conjunction with the absence of diffusion of electroactive material from the bulk solution, results in greater resolution of poorly separated waves than can be achieved in diffusion-controlled experiments such as cyclic voltammetry. (The shape of the thin layer voltammetric wave will be shown to be identical to that obtained in ac

voltammetry, the latter technique being noted for its ability to resolve closely spaced charge transfer processes (4).) The short time required for complete electrolysis makes thin layer techniques particularly powerful for the determination of the stoichiometry of complex electrode reactions.

Thin layer electrodes in general suffer from problems associated with uneven potential distribution across the electrode surface (5). This arises from the high resistance presented to the flow of current through thin layers of solution with small cross-sectional areas. Even in highly conductive aqueous media, the potential distribution is such that agreement between theory and experiment is seldom excellent. As a result, examples of the application of thin layer techniques to the determination of, for instance, heterogeneous kinetic parameters, are rare. Cells have been designed utilizing conductive membranes (6) to provide a uniform current path between the counter and working electrodes, and these alleviate, to a large extent, the problem of uneven potential distribution. These are difficult to construct, however, and have not found common usage.

In non-aqueous solvent/electrolyte systems, solution resistivities as high as 3000 ohm-cm (7) may be encountered. The resulting potential distribution problems are particularly severe, and it has been suggested (5) that implementation of thin layer methodology, even in solvents of relatively high dielectric constant, such as acetonitrile or dimethylformamide, would be difficult. It is in such poorly conducting media that the advantages of thin-layer methodology may often be most

beneficial, however.

In this paper the application of thin layer voltammetry in non-aqueous media is considered. The discussion is centered around immersed thin layer electrodes, i.e. those in which the edges of the thin layer cavity are immersed in bulk solution, since a greater cross sectional area is available for the flow of current, and the resulting potential distribution is therefore less severe.~~(8)~~[2] Such cell designs always suffer to some extent from diffusion of electroactive material from the bulk solution into the thin layer cavity, but it will be demonstrated experimentally that this does not seriously affect the usefulness of results. Experimental verification and practical cell design are treated in part II (9).

Linear Sweep Voltammetry at Thin Layer Electrodes

The theory and application of thin layer voltammetric methods has been reviewed in detail (3). The most commonly used technique is that of linear sweep voltammetry. Here, a linearly increasing potential is applied to the working electrode and the resulting current is recorded as a function of the applied potential. In the cyclic version of this technique, the direction of the potential scan is reversed once some predefined switching potential is reached, and recording of the current is continued while the potential is linearly scanned back to its initial value.

If the thickness of the thin layer of solution next to the working electrode is sufficiently small, and if the rate, dE/dt

= ν, at which the applied potential is varied is sufficiently slow, then all species may be considered to be uniformly distributed throughout the thin layer cavity. Given the generalized reversible electrode reaction

$$Ox + ne^- \rightleftharpoons Red$$

and the above conditions, the current resulting as the potential is scanned from a value where one form of the redox couple predominates to a point where the other form is favored is given by

$$i = \frac{(nF)^2 V \nu C_{Ox}^0 \exp[(nF/RT)(E-E^0)]}{RT[1 + \exp[(nF/RT)(E-E^0)]^2} \qquad [1]$$

as first derived by Hubbard and Anson (10). Here, V is the volume of the thin layer next to the electrode surface, and C_{Ox}^0 is the bulk concentration of the electroactive species. Other notation is conventional. This equation describes a Gaussian shaped curve with the peak current occurring at E° and given by

$$i_p = \frac{(nF)^2 V \nu C_{Ox}^0}{4RT} \qquad [2]$$

The second order dependence of the peak current on the number of electrons makes equation [2] particularly attractive for n-value determination.

A voltammetric criterion allowing for the determination of n without prior knowledge of C_{Ox}^0 or V may be readily derived.

One-half of the peak current is given by

$$i_{p/2} = \frac{(nF)^2 V \nu C_{Ox}^0}{8RT}$$

Substitution of this current into equation [1] and solving for $(E-E^\circ)$ leads to the quadratic expression

$$a^2 - 6a + 1 = 0$$

where

$$a = \exp[(nF/RT)(E-E^\circ)]$$

At 25°C this gives

$$E-E^\circ = \frac{\pm 45}{n} \text{ mV} \qquad [3]$$

The width of the peak at half-height is therefore given by

$$E_{0.5h} = \frac{90}{n} \text{ mV} \qquad [4]$$

This result has apparently not appeared in the literature, but should provide a rapid and convenient means for estimating n. (The same expression for the width at half-height and the same second order dependence of the peak height on n apply to the reversible ac voltammetric wave (11).)

More rigorous derivations of the linear sweep thin layer

voltammetric response, taking into account the diffusion of electroactive species within the thin layer cavity, have appeared (10). The resulting equations are cumbersome and have not found common use. Provided the thin layer thickness is of the order of 10 μm or less, the results of this treatment do not differ significantly from the predictions of eqn. [1] when the potential sweep rate is 10 $mV\text{-}s^{-1}$ or less. The effects of solution resistance, and the resulting uneven potential distribution, on the linear sweep voltammetric response have not previously been considered quantitatively. Experimentally, however, some degree of asymmetry in the peaks is always observed, and anodic peak potentials are displaced to positive values while the reverse is observed for cathodic peaks.

Effects of Solution Resistance on the Thin Layer Voltammetric Response

The model used here to describe the potential distribution in thin layer cells was first used by Goldberg, *et. al.* to describe resistive effects in combined esr-electrochemical cells (12), and in thin layer cells (6), during current and potential step experiments. It has not, however, been used to describe resistive effects during potential sweep experiments, or to predict the extent to which cell geometry might determine the magnitude of such effects.

Two types of cell geometry will be considered here. The first, Figure 1, consists of a square or rectangular metallic electrode surface placed in a plane parallel to an insulating

surface. The two surfaces are separated by a distance l, equal to the thickness of the thin layer cavity. Three of the edges of the electrode are considered insulating, and the fourth edge is equidistant from a secondary electrode placed within the cavity such that uniform parallel current flow between the secondary electrode and the exposed edge of the working electrode may be assumed. The working electrode potential is sensed via a Luggin capillary placed between the secondary and working electrodes. This geometry corresponds to that found in conventional optically transparent thin layer electrodes (OTTLE's), where the working electrode, generally a platinum or gold mini-grid, Figure 2, is transparent to the passage of light.

The second geometry, Figure 3, corresponds to the type of immersed thin layer electrode (ITLE) first used by Oglesby et. al. (8). The working electrode surface is a planar disc, and a radially uniform current path is provided between the edges of the disc and a secondary electrode arranged concentric to the disc.

The model used herein to discuss the potential distribution across the working electrode considers that the thin layer cavity next to the working electrode may be divided into a number of volume increments, each successive increment being displaced a distance dx from the capillary tip. As the volume increments lie at successively greater distances from the Luggin, successively greater solution resistances are presented to the current flowing into each increment. In the OTTLE geometry, the volume of each increment is constant, and given by wldx, where w is the length

of the exposed edge of the working electrode. The individual resistances separating the volume increments are also constant, and may be calculated from

$$R_i = \rho\, dx/lw \qquad [5]$$

where ρ is the specific resistivity of the solvent/electrolyte system. The uncompensated resistance, $R_u = R_1$, between the Luggin tip and the first volume increment is given by eqn. [5] where dx is now the distance between the Luggin tip and the edge of the working electrode.

In the concentric radial geometry, the volume of each increment is that contained between two concentric cylinders of radii r and r-dr, and may be calculated from

$$V_i = \pi\, l(2r_i dr - dr^2) \qquad [6]$$

where r_i is the outer radius of V_i. As the radii of the volume increments decreases, so does the cross-sectional area available for the flow of current. The resistance increments between successive volumes therefore must increase as the radii of the volume increments decrease. The resistances can be calculated with reference to Figure 4. If the difference dr between the radii, r_i and r_{i-1}, of two cylinders is infinitesimal, then the resistance to current flow between the two cylinders is given by

$$R = \rho dr/2\pi rl$$

If dr is no longer required to be infinitesimal, then the resistance between the two cylinders will be given by

$$R_i = \int_{r_i}^{r_{i-1}} \frac{\rho dr}{2\pi r l}$$

or

$$R_i = (\rho/2\pi l) \ln(r_{i-1}/r_i) \qquad [7]$$

The effective potential at each of the volume elements may be calculated once the volumes of the individual elements and the resistances between them are known. With reference to Figure 5, depicting the case for the radial concentric cell geometry, suppose that the total current flowing into the thin layer cavity is i_t. If the applied potential, <u>i.e.</u> that appearing at the Luggin tip, is E_{app}, then the potential appearing at the first volume increment is given by

$$E_1 = E_{app} - i_t R_1 \qquad [8]$$

The current, i_1, flowing into the first volume element may now be calculated from eqn. [4] by setting $V = V_1$ and $E = E_1$. Now, if n volume elements are assumed, the current flowing through R_2 is given by

$$i_t - i_1 = \sum_{i=2}^{n} i_i$$

and the potential appearing at the second volume increment is

$$E_2 = E_1 - R_2 \sum_{i=2}^{n} i_i$$

With knowledge of E_2 and V_2, the current i_2 is obtained, and so on until all of the individual potentials and currents have been obtained. Noting that

$$\sum_{j=i}^{n} i_j = i_t - \sum_{j=1}^{i-1} i_j \qquad [9]$$

the equation

$$E_i = E_{i-1} - R_i(i_t - \sum_{j=1}^{i-1} i_j) \qquad [10]$$

may be applied generally to determine the potential distribution in thin layer cells.

An iterative procedure based on equation [10] has been developed here to allow numerical calculation of thin layer voltammograms. Equation [1] is used to provide an initial estimate, i_t, of the total current flowing to the thin layer electrode. Equation [10] is then used as described above to calculate the potentials and currents associated with the individual volume elements. If the initial estimate agrees within 0.1% of the sum of the individual currents, it is assumed to be correct. If it does not, a new estimate is calculated according to

$$i_t' = i_t - C$$

where C is a small value of appropriate sign calculated within the program on the basis of the difference between the initial estimate and the sum of the individual currents. The procedure is then repeated until the desired degree of convergence is obtained.

In general, twenty volume increments were used for the calculations. In no case, however, was a significant difference in the results observed upon decreasing the number of elements to 10.

The program has been used to predict the effects of various prameters on the resistance induced asymmetry of the thin layer voltammetric waves. The results are presented in Figures 6 to 10. All of the curves are anodic, and the potential is scanned from left to right. The potential scan rate assumed in all cases is 5 $mV\text{-}s^{-1}$, the thickness of the thin layer is 10 μm, and the concentration of electroactive species is 1 mM. Other parameters listed in the figures are as follows: dref is the distance between the Luggin tip and the edge of the working electrode, ρ is the solution resistivity, r is the radius of the working electrode in the concentric radial configuration, and w and h are the width and length of the working electrode in the OTTLE configuration, w being considered parallel to the secondary electrode. In all of the figures the central curve, marked a, is that calculated directly from eqn. [1] assuming zero solution resistance. For purposes of comparison and clarity, all other

curves are normalized to this one.

Figure 6 illustrates some results calculated for the OTTLE configuration. The solution resistance used here, ρ = 250 ohm-cm, corresponds roughly to that expected (7) for the commonly used solvent/electrolyte system CH_3CN/0.1 M tetrabutylammonium perchlorate (TBAP). The resistive potential drops in this case occur along the dimension h, and this parameter therefore determines the degree to which the curves are affected by ohmic polarization. The dimension h in Figure 6 is 0.354 cm, and is much less than that used in most conventional OTTLE designs. The effect of the solution resistance can be reduced dramatically by decreasing h, as shown in Figure 6b, where this dimension has been halved. The same effect can be achieved by using two counter electrodes placed parallel to and at equal distances from opposite edges of the working electrode. A similar design has been employed by Goldberg et. al. (13) in combined esr-electrochemical experiments.

Figure 7 compares the results of the calculation for the OTTLE configuration with those obtained for a radial concentric geometry where the area of the two working electrodes, and all other parameters, are identical. This figure clearly illustrates the superiority of the radial configuration. In comparing Figures 6b and 7b, it is evident that the radial configuration should provide better results than an OTTLE cell of half the working electrode area. Geometry is clearly an extremely important factor in thin layer electrochemical cell design. It should be pointed out here that the radial design can be readily

modified to serve as a reflectance cell for modulated specular reflectance (MSRS) experiments.

Figures 8 and 9 illustrate the effects of varying the solution resistivity and the electrode radius, respectively, for the radial configuration. In comparing the two figures it is evident that, at least for radii in the 2 to 4 mm range and solution resistivities in the 300 ohm-cm vicinity, decreasing the electrode radius by 1 mm has very nearly the same effect as decreasing the solution resistivity by 100 ohm-cm. Thus, when forced to work in highly resistive media, smaller electrodes should give better results. It should be noted, however, that diffusion of electroactive material into the thin layer cavity, which has been ignored in these calculations, will become more important as the electrode radius is decreased. There will therefore be a limit, dictated largely by the ratio of the electrode area to the thickness of the thin layer cavity, to how small a practical electrode may be made.

Figure 10 illustrates the effects of displacing the Luggin tip to greater distances from the edge of the working electrode. The magnitude of the uncompensated resistance, R_u, apparently has little effect on the magnitude of the peak currents, but does introduce substantial asymmetry into the voltammetric waves. Placement of the Luggin capillary is an important consideration in the design of any electrochemical cell.

The program predicts that the thickness of the thin layer cavity has no effect on the normalized current-voltage curves.

This result is readily predictable. While the individual resistance increments decrease in direct proportion to an increase in the thin layer thickness, the individual volumes, and hence the currents, increase. The individual iR potential drops across the working electrode therefore remain constant, and the potential distribution is unaffected.

The effect of other factors which affect the magnitude of the current, but not the resistance increments, can be readily predicted. Hence, an increase in either the sweep rate ν or the concentration of electroactive species will result in an increase in current, and a corresponding deterioration in the quality of the voltammograms will be observed. Many of these points are clearly illustrated in part II (9).

ACKNOWLEDGEMENT

The authors thank the Office of Naval Research, Washington, for support of part of this work. One of us (A.S.H.) thanks the Alberta Heritage Foundation for Medical Research for financial support.

REFERENCES

1. A.J. Bard and L.R. Faulkner, "Electrochemical Methods", John Wiley and Sons, New York, 1980

2. A.J. Bard and K.S.V. Santhanam, in "A.J. Bard, ed., "Electroanalytical Chemistry", vol. 4, Marcel Dekker, New York, 1970, pp 215-315.

3. A.T. Hubbard and C.F. Anson, ibid, pp 129-214.

4. B. Bryer and H.H. Bauer in P.J. Elving and I.M. Kolthoff, eds. "Chemical Analysis", vol. 13, Wiley Interscience, New York, 1963.

5. I.P. Goldberg and A.J. Bard, J. Electroanal. Chem. 38, 314 (1972).

6. G.M. Tom and A.T. Hubbard, Anal. Chem. 43, 671 (1971).

7. D.T. Sayer and J.L. Roberts, Jr., "Experimental Electrochemistry for Chemists", Wiley Interscience, New York, 1974.

8. D.M. Oglesby, S.H. Omang, and C.N. Reilly, Anal. Chem. 37, 312 (1965).

9. A. Scott Hinman, Stanley Pons, and John Cassidy (Part II)

10. A.T. Hubbard and F.C. Anson, Anal. Chem. 38, 58 (1966).

11. D.E. Smith in A.J. Bard, "Electroanalytical Chemistry", vol. 1, Marcel Dekker, New York, 1966, pp. 1-155.

12. I.B. Goldberg, A.J. Bard, and S. Feldberg, J. Phys. Chem. 76, 2550 (1972).

13. I.B. Goldberg and A.J. Bard, J. Phys. Chem. 75, 3281 (1971).

FIGURE LEGENDS

Figure 1. Geometry of rectangular thin layer electrode.

Figure 2. Optically transparent thin layer electrode.

Figure 3. Concentric radial thin layer electrode geometry.

Figure 4. Solution resistance in concentric radial thin layer electrodes.

Figure 5. Model for the potential distribution at thin layer electrodes.

Figure 6. Effect of increasing vertical dimension of the working electrode in the OTTLE configuration:

ρ = 250 Ω-cm; dref = 0.1 cm; w = 0.354 cm;

(a) theoretical response with ρ = 0

(b) h = 0.177 cm

(c) h = 0.354 cm

Figure 7. Comparison of the resistive effect on calculated voltammograms at OTTLE (c) and radial (b) thin layer electrodes of equal area: ρ = 250 Ω cm; dref = 0.1 cm.

(a) theoretical response with ρ = 0

(b) r = 0.2 cm

(c) h = w = 0.354 cm

Figure 8. Effect of solution resistance on calculated voltammograms at radial thin layer electrode: r = 0.4 cm; dref = 0.1 cm

(a) theoretical response with ρ = 0

(b) ρ = 100 Ω-cm

(c) ρ = 200 Ω-cm

(d) ρ = 300 Ω-cm

Figure 9. Effect of electrode radius on calculated voltammograms at radial thin layer electrode:

ρ = 250 Ω-cm; dref = 0.1 cm.

(a) theoretical response with ρ = 0

(b) r = 0.2 cm

(c) r = 0.3 cm

(d) r = 0.4 cm

Figure 10. Effect of displacing Luggin capillary on calculated thin layer voltammograms at radial thin layer electrode: ρ = 250 Ω-cm; r = 0.2 cm.

(a) theoretical response with ρ = 0

(b) dref = 0.1 cm

(c) dref = 0.5 cm

(d) dref = 1.0 cm

(e) dref = 1.5 cm

END

FILMED

1-85

DTIC